Electrochemical Polymerization of 2-Phenylindole and Characterization of Its Polymer

Yuzhen Li,[1] Jinguo Cui,[1,2] Houting Liu,[1] Yi Rao,[2] Jingkun Xu,[1] Jian Hou[3]

[1]*Jiangxi Key Laboratory of Organic Chemistry, Jiangxi Science and Technology Normal University, Nanchang 330013, Jiangxi Province, People's Republic of China*
[2]*Jiangxi University of Traditional Chinese Medicine, Nanchang 330006, Jiangxi Province, People's Republic of China*
[3]*State Key Laboratory for Marine Corrosion and Protection, Luoyang Ship Material Research Institute, Qingdao 266071, Shandong Province, People's Republic of China*

Received 3 April 2008; accepted 21 December 2008
DOI 10.1002/app.29957
Published online 13 March 2009 in Wiley InterScience (www.interscience.wiley.com).

ABSTRACT: High-quality poly(2-phenylindole) (PPI) films were synthesized electrochemically by direct anodic oxidation of 2-phenylindole (PI) in boron trifluoride diethyl etherate (BFEE). The onset oxidation potential of PI in this medium was measured to be only 0.83 V versus a saturated calomel electrode (SCE), which was much lower than that determined in acetonitrile (ACN) containing 0.1 mol L^{-1} tetrabutylammonium tetrafluoroborate (1.05 V vs. SCE). PPI films obtained from BFEE showed good electrochemical behavior and thermal stability with an electrical conductivity of 10^{-2} S cm^{-1}. Structural studies showed that the polymerization of PI mainly occurred at the 3,6-positions. As-formed PPI films could be partly dissolved in dimethyl sulfoxide. Fluorescence spectral studies indicated that PPI was a blue-green light emitter.
© 2009 Wiley Periodicals, Inc. J Appl Polym Sci 113: 96–103, 2009

Key words: conducting polymers; polyindoles; boron trifluoride diethyl etherate; electrochemical polymerization

INTRODUCTION

The pursuit of high-quality conducting polymer films is still one of the main goals in the research and development of inherently conducting polymers (CPs) because of their potential applications.[1–4] Among the CPs investigated during the past 10 years, polyindole and its derivatives have attracted remarkable interests[5–16] because of their fairly good thermal stability, high redox activity and stability,[9–12] slow degradation rate in comparison with those of polyaniline and polypyrrole,[11] and air-stable electrical conductivity in the doped state.[13] Polyindoles may be good candidates for applications in electrochemical sensors, electrocatalysis, mild steel protection, and biological areas.[17] For many of these applications, it is desirable to produce electroactive polyindole layers with a wide variety of substituents.

However, there still exists some uncertainty concerning the position of the coupling sites of indole [Scheme 1(A)] and its derivatives [Scheme 1 (B) and (C)]. Waltman et al.[18] reported that the monomers are coupled through 1,3-positions, whereas Zotti et al.[19] reported the coupling through 2,3-positions. In our previous papers,[20,21] we reported that the coupling between the monomer units mainly occurred at the C_2 and C_3 positions of indole and its derivatives.

To learn more about the electropolymerization reaction of indole and its derivatives, we chose PI [Scheme 1(C)], a new monomer which C_2—H was substituted by the phenyl group. This article mostly studied on whether this new monomer can be polymerized and the properties of as-formed poly(2-phenylindole) (PPI) films and the coupling sites of PI.

On the other hand, BFEE is an excellent electrolyte, and no other supporting electrolyte is needed for the electrochemical polymerization of aromatic compounds, such as benzene and thiophene.[22–27] High-quality free-standing CP films can be achieved in this electrolyte. Our previous studies have shown that high-quality free-standing polyindole and its derivative films can also be easily electrodeposited from BFEE,[20,21] in good agreement with high-quality CP film formation in this medium, such as polythiophenes,[28] polypyrrole,[29–31] polyfuran,[32,33] and poly(*para*-phenylene).[34] Up to now, there have been no reports on the electropolymerization of PI in BFEE-based electrolytes.

In this study, high-quality PPI films were easily prepared by the anodic oxidation of PI monomer

Correspondence to: J. Xu (xujingkun@mail.ipc.ac.cn or xujingkun@tsinghua.org.cn).
Contract grant sponsor: NSFC; contract grant number: 50663001.
Contract grant sponsor: Ministry of Education of China; contract grant number: 2007–207058.

© 2009 Wiley Periodicals, Inc.

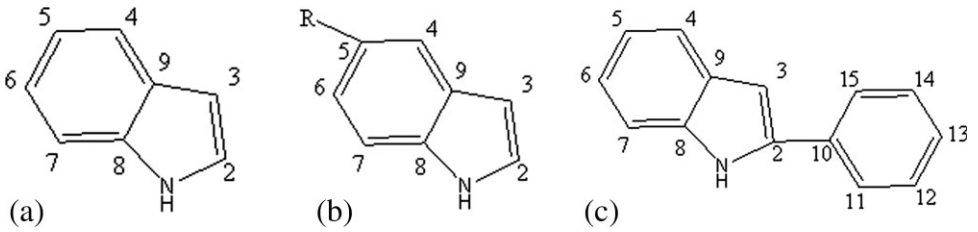

Scheme 1 The chemical structure of indole(A), 5-substituted indole(B), and PI(C).

directly in BFEE. The electrochemical properties, polymerization mechanism, thermal stability, fluorescence properties, and morphology of as-prepared PPI films were studied in detail.

EXPERIMENTAL

Materials

BFEE (1.12–1.14 × 10^3 g L^{-1}, BF_3 = 48.24%; Beijing Changyang Chemical Plant, Beijing, People's Republic of China) was distilled and stored at –20°C before use. PI (99%; Acros Organics, USA) and commercial high-performance liquid chromatography grade acetonitrile (ACN; Tianjin Guangfu Fine Chemical Research Institute, Tianjin, People's Republic of China) were used directly without further purification. Tetrabutylammonium tetrafluoroborate (Bu_4NBF_4, 95%; Acros Organics) was dried under vacuum at 60 °C for 24 h before use.

Apparatus

The electrical conductivity of PPI films was measured by the conventional four-probe technique with pressed pellets of the sample.[35] The arrangement of four probes is shown in Scheme 2. The current (I) was applied by two probe of a model 263 potentiostat–galvanostat (EG & G Princeton Applied Research) under a computer control at 1 and 4, and the voltage (V) between 2 and 3 is measured by a multimeter. The space between 2 and 3 is L and T, and φ denote the width and thickness of sample, respectively. Then, the electrical conductivity (σ) of sample is calculated according to the well-known equation given as follows:

$$\sigma = \frac{1}{U} \times \frac{1}{T\phi} \tag{1}$$

UV–visible spectra were taken by using a Perkin–Elmer Lamda 900 UV–vis–NIR spectrophotometer. Fourier transform infrared (FTIR) spectra were recorded by using KBr pellets of the polymers on the Bruker Vertex 70 FTIR spectrometer. The fluorescence spectra were determined with an F-4500 fluorescence spectrophotometer (Hitachi). The thermogravimetric (TG) and differential thermogravimetric (DTG) analyses were performed with a thermal analyzer of Netzsch TG209. Scanning electron microscopy (SEM) measurements were taken by using a JEOL JSM–6360 LA analytical scanning electron microscope. The fluorescence quantum yield (φ) of PPI in solution was measured using anthracene in ACN (standard, $\varphi_{ref} = 0.27$)[36] as a reference and were calculated according to the well-known method given as follows:

$$\phi_{\text{overall}} = \frac{n^2\, A_{\text{ref}}\, I}{n_{\text{ref}}^2\, A\, I_{\text{ref}}}\, \phi_{ref} \tag{2}$$

here, n, A, and I denote the refractive index of the solvent, the absorbance at the excitation wavelength, and the intensity of the emission spectrum, respectively. The subscript "ref" denotes the reference, and no subscript denotes the sample. Absorbance of the samples and the standard should be similar.[37]

Electrochemical tests and polymerization

The electrochemical experiments were performed in a one-compartment cell by the use of a Model 263A potentiostat–galvanostat (EG & G Princeton Applied Research) under a computer control. For electrochemical examinations, the working and counter electrodes were a Pt wire with diameter of 0.5 mm and a stainless steel wire with diameter of 1 mm, respectively. They were placed 5 mm apart during

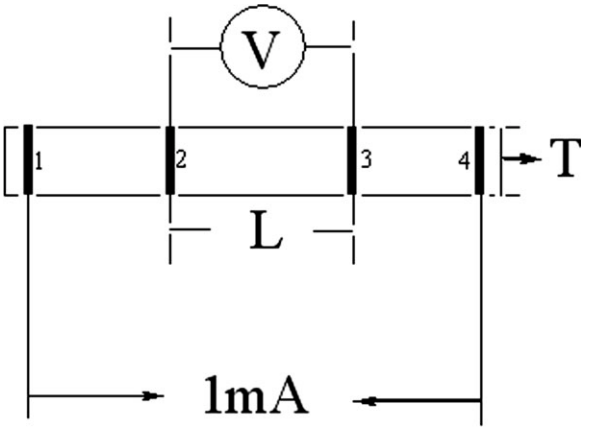

Scheme 2 The sketch map of four-probe technique.

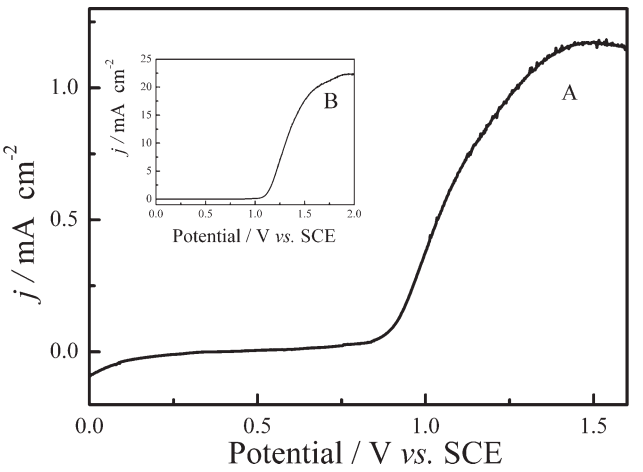

Figure 1 Anodic polarization curves of PI in BFEE (A) and ACN + 0.1 mol L^{-1} Bu_4NBF_4 (B). Potential scan rates: 100 mV s^{-1}.

the experiments. Previous studies had demonstrated that both the stainless steel sheet and BFEE were electrochemically inert during the electrochemical polymerization process.[38] Therefore, for large amount of polymer film growth, the working and counter electrodes were two stainless steel sheets (AISI 304, 10 mm × 20 mm) placed 10 mm apart. Before the polymerization, they were carefully polished with abrasive paper (1500 mesh) and cleaned with water and acetone successively, and then dried by a blower. All potentials have been calibrated to saturated calomel electrode (SCE).

The typical electrolyte solution is freshly distilled BFEE containing 0.1 mol L^{-1} PI. All solutions were deaerated by a dry argon stream for 10 min before each experiment and a slight argon over pressure was maintained during the experiments.

RESULTS AND DISCUSSION

Electrochemical synthesis of PPI films

The anodic polarization curves of PI in BFEE and in ACN containing 0.1 mol L^{-1} Bu_4NBF_4 are shown in Figure 1. The oxidation onset of PI was initiated at 0.80 V versus SCE in BFEE, which was much lower than that of PI in ACN containing 0.1 mol L^{-1} Bu_4NBF_4 (1.08 V vs. SCE, Fig. 1 inset). Generally, lower oxidation potential onset can lead to easier oxidation of the monomers at given applied potential. In addition, after the polarization process, a black polymer film can be found on the working electrode in BFEE, whereas no deposits can be found in ACN solution. This result clearly indicated that the oxidation of PI in BFEE was much easier than in ACN containing 0.1 mol L^{-1} Bu_4NBF_4, and BFEE may be a suitable medium for the electropolymerization of PI.

The successive cyclic voltammograms (CVs) of 0.1 mol L^{-1} PI in BFEE and ACN on Pt electrode are shown in Figure 2, respectively. In BFEE [Fig. 2(A)], the CVs of PI showed characteristic features of other CPs or oligomers, which we reported previously during potentiodynamic syntheses, such as pyrene,[39] 1-nitropyrene,[40] 9,10-dihydrophenanthrene,[41] and benzanthrone,[42] and so on. In the first cycle, the anodic current began to increase at 0.80 V versus SCE, and there was a current loop between 0.80 V and 1.43 V versus SCE. The formation of this loop is characteristic of nucleation processes, as reported in the literature.[42] During the experiments, it was also found that a shiny, compact, and homogeneous PPI film black in color on the Pt electrode surface was formed gradually at potentials greater than 0.80 V versus SCE. As the potential scanning continued, there was an obvious reduction peak near 0.47 V versus SCE. The redox peaks were attributed to the p-doping/dedoping processes of the PPI film formed in previous potential scans. From the figure, the increases of the redox wave currents implied that the amount of the polymer deposited on the electrode increased cycle by cycle. Moreover, the obvious potential shift of the wave current maximum provides information about the increase in the electrical resistance in the polymer film and the overpotential needed to overcome the resistance. All these phenomena indicated that a high-quality conducting PPI film was formed on the working electrode in BFEE. Furthermore, further research proved that the redox currents kept increasing until the cycle number reached 170 or so. After that, the redox current became almost stable and the wave

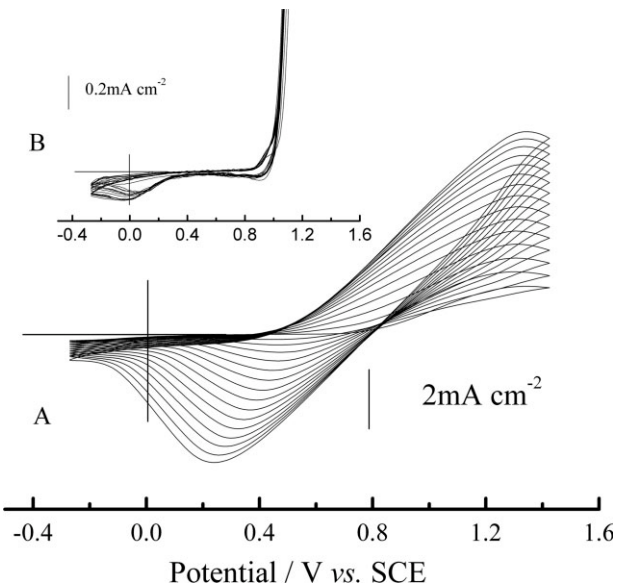

Figure 2 CVs of 0.1 mol L^{-1} PI in BFEE (A) and ACN + 0.1 mol L^{-1} Bu_4NBF_4 (B). Potential scan rates: 100 mV s^{-1}.

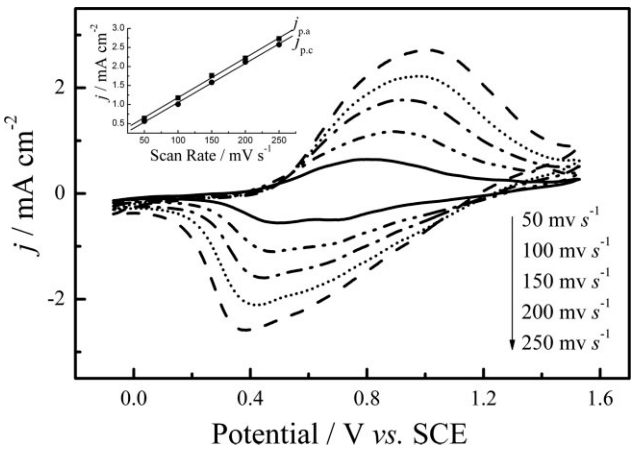

Figure 3 CVs of PPI films in BFEE at potential scan rates of 50, 100, 150, 200, and 250 mV s^{-1}. The polymer film was synthesized electrochemically in BFEE at a constant applied potential of 1.23 V versus SCE.

current maximum performed a contrary potential shift. This implies that the amount of the polymer films deposited on the electrode is so thick that it prevents the moving in/out of the dopants during the redox process in the polymer. On the other hand, the CVs of PI in ACN under similar conditions were not satisfactory [Fig. 2(B)]. There was no polymer film formed on the working electrode surface, although a reduction peak appeared approximately at 0.06 V versus SCE. On the basis of these discussions, BFEE was a more suitable medium than ACN for the electrosynthesis of high-quality PPI films. Therefore, the following experiments were mainly performed in BFEE.

Electrochemistry of PPI films

The electrochemical behavior of the PPI films deposited electrochemically from BFEE was studied in monomer-free BFEE (Fig. 3). Similar to the results reported in the literature,[39–43] the steady-state CVs represent broad anodic and cathodic peaks in monomer-free BFEE. The peak current densities were proportional to the potential scanning rates (Fig. 3, inset), indicating the reversible redox behavior of the polymer.[44,45] Furthermore, these films could be cycled repeatedly between the conducting (oxidized) and insulating (neutral) state without significant decomposition of the materials, indicating the high structural stability of the polymer. Additionally, from the figure, it can be clearly seen that the polymer films could be oxidized and reduced from 1.01 V (anodic peak potential, E_a) to 0.38 V versus SCE (cathodic peak potential, E_c) in monomer-free BFEE. On the basis of the previous discussions, it can be reasonably concluded that PPI films electrodeposited from BFEE showed good redox activity and stability.

Structural characterization

During the potentiostatic deposition of PPI in BFEE, the electrolyte solution was very stable, and its color changed very slowly from slight yellow to yellow. This indicated that partly soluble oligomers were formed during the oxidation and diffused away from the electrode into the bulk solution. However, high-quality PPI films still can be formed on stainless steel sheet.

The PPI films from BFEE can be partly dissolved in strong polar solvents such as DMSO and cannot be dissolved in common organic solvents such as tetrahydrofuran, acetone, CH_2Cl_2, etc. As-prepared PPI films consist of polymers and oligomers containing various quantities of monomer units and different degrees of polymerization. The part that can dissolve in DMSO was mainly oligomers with short chain length, whereas the components of the residual polymers usually have longer conjugated length and larger molecular weights. The UV–vis spectra of PI (A), soluble doped PPI (B), and soluble dedoped PPI (C) dissolved in DMSO were examined, as shown in Figure 4. The UV–vis spectra of both doped and dedoped PPI films were quite similar in DMSO solution mainly owing to the auto-dedoping of PPI films. In addition, the UV–vis spectrum of doped PPI on ITO electrode was also tested and it is also very similar to those in DMSO. The color of PPI film was dark green when taken out of the BFEE solution. After about several minutes, it changed quickly to bronze. This phenomenon was mainly due to the easy self-dedoping of PPI in solvent or air because BFEE as the dopant can react with the moisture in the air easily and quickly. It can be clearly seen from Figure 4 that PI monomer showed the

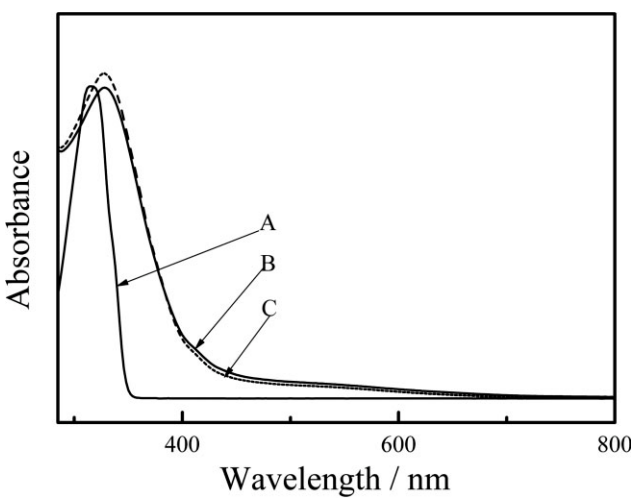

Figure 4 UV–vis spectra of PI monomer (A), doped PPI (B), and dedoped PPI (C) films. PPI films were prepared potentiostatically at 1.23 V versus SCE from BFEE. Solvent: DMSO.

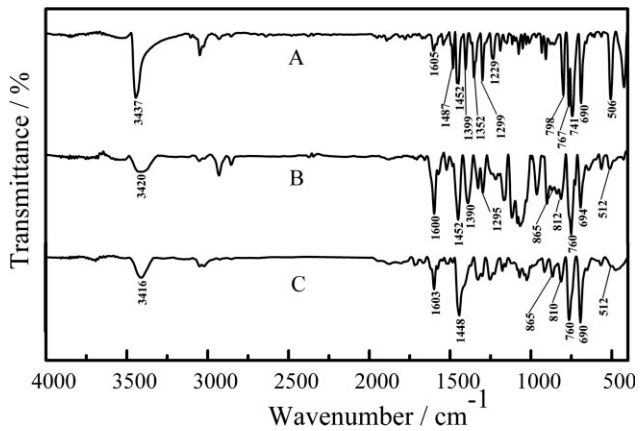

Figure 5 FTIR spectra of PI monomer (A), doped PPI (B), and dedoped PPI (C) films. PPI films were prepared potentiostatically at 1.23 V versus SCE from BFEE.

absorption maximum at 315 nm. However, the spectra of the doped and dedoped PPI films showed broad absorption with an absorption maximum at 327 nm. The overall absorption tails off to about 800 nm. Generally, the red shift in the UV spectra means the increase of the conjugated link. Therefore, these results confirmed the formation of a conjugated polymer.

The FTIR spectra of PI and PPI films prepared potentiostatically in doped and dedoped states are shown in Figure 5(A– C), respectively. The strong and narrow peak at 3437 cm^{-1} observed in the PI spectrum is the characteristic absorption of the N—H bond, which is shifted to 3420 and 3416 cm^{-1} in the spectrum of the doped and dedoped PPI films. This band, together with the band at 1605 cm^{-1}, can be ascribed to the elongation and the deformation vibrations of the N—H bond, respectively. This result implies that there are still N—H bonds on the doped and dedoped PPI main chains. Therefore, nitrogen species could not be the polymerization sites. According to the literature, there are two main opinions on the electrochemical polymerization mechanism of indole and its derivatives: 1,3-positions or 2,3-positions. The presence of the N—H bonds on the doped and dedoped PPI films showed that the 1-position is not the polymerization site. Meanwhile, 2-position is also not the polymerization site because C_2—H was substituted by the phenyl group. The peak located at 1487 cm^{-1} was assigned to the stretching of the benzene ring. The peak of 741 cm^{-1} is characteristic of the out-of-plane deformation of C_8 and C_9 *o*-disubstituted in the spectrum of the monomer. On the contrary, its disappearance and the peaks of 865 cm^{-1} and 812 cm^{-1} could be explained by C_6, C_8, and C_9 trisubstitution in the polymer. Therefore, this implied that C_6 may be the coupling sites.

To get deep insight into PPI structure and the polymerization mechanism, the atomic electron density population and reactivity of PPI were also calculated by the B3LYP/6–31G (d,p) level using Gaussian03 software.[46] The results of main atomic electron density populations showed negative electric charges on N_1, C_3, C_4, C_6, C_7, C_{11}, and C_{15} (Table I), which implied that these atoms will donate electrons during the electrochemical polymerization of PPI through radical cations intermediates. According to the molecular orbital theory, the reaction between the active molecules mainly happens on the frontier molecular orbital and near orbital. For PI, the proportions of atoms C_2, C_3, and C_6 in HOMO were higher than other atoms, as listed in Table II. All of these demonstrated that C_3 could be a coupling site. Combining the results of main atomic electron density populations, the theoretical results implied that the polymerization sites between the monomer could occur preferentially at C_3 and C_6, in well accordance with the IR results.

TABLE I
Main Atomic Electron Density Populations for 2-Phenylindole

Atom	Electric charge	Atom	Electric charge
$N_{(1)}$	−0.675002	$C_{(2)}$	0.248529
$C_{(3)}$	−0.180805	$C_{(4)}$	−0.146279
$C_{(5)}$	−0.093906	$C_{(6)}$	−0.105222
$C_{(7)}$	−0.108074	$C_{(8)}$	0.307694
$C_{(9)}$	0.075914	$C_{(10)}$	0.093470
$C_{(11)}$	−0.110591	$C_{(12)}$	−0.092951
$C_{(13)}$	−0.083129	$C_{(14)}$	−0.088201
$C_{(15)}$	−0.127165		

The fluorescence spectra of PI and dedoped PPI prepared in BFEE were examined, using DMSO as the solvent, through the wavelength scans of excitation and emission as shown in Figure 6. The excitation spectrum of the PI monomer was mainly located at 273 and 346 nm, whereas the emission peaks were at 371 nm. On the contrary, the excitation spectrum of dedoped PPI can be found at 383 nm, whereas its emission spectrum obviously appeared at 461 nm. This implies that there is a large bathochromic shift of both the excitation and emission spectra between the monomer and the polymer. The wide peak distribution can be ascribed

TABLE II
Main Composition and Proportion of the Frontier Orbitals in 2-Phenylindole PI (%)

Atom	HOMO-1	HOMO	LUMO	LUMO+1
$N_{(1)}$	23.5920	5.3673	6.1936	3.4994
$C_{(2)}$	2.3639	18.3164	11.3335	10.2725
$C_{(3)}$	3.0779	22.0333	12.6723	2.6893
$C_{(4)}$	7.0279	11.2530	10.6381	0.0551
$C_{(5)}$	23.3213	0.0492	1.0902	0.2612
$C_{(6)}$	1.2161	14.5563	8.4736	0.1422

to the wide molar mass distribution of PPI. The fluorescence quantum yield of dedoped PPI in DMSO was measured to be 0.1 according to eq. (1). All these results demonstrated that the polymer is a blue-green light emitter and may have some potential applications in organic optoelectronics.

Thermal analylsis

The thermal stability of CPs is very important for their potential applications. TGA is a significant dynamic way of detecting the degradation behaviors. The weight loss of a polymer sample is measured continuously, whereas the temperature is changed at a constant rate. To investigate the thermal stability of PPI films prepared from BFEE, the thermal analysis of dedoped PPI films was tested, as shown in Figure 7. The thermal analysis was performed under a nitrogen stream in the temperature

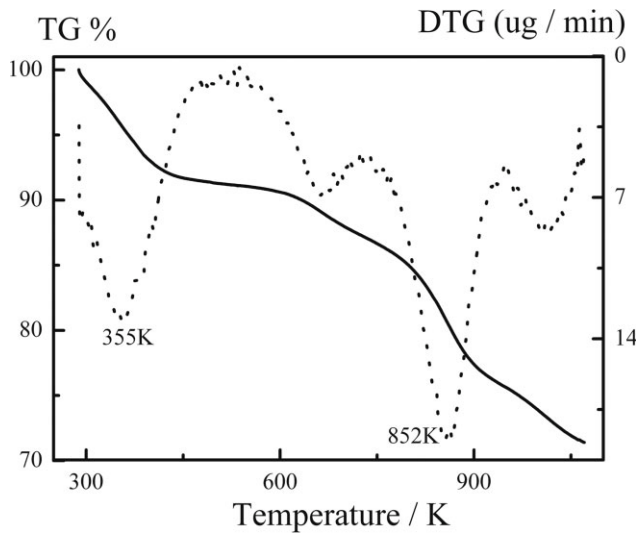

Figure 7 TG/DTG curves of dedoped PPI films obtained potentiostatically at 1.23 V *vs.* SCE from BFEE.

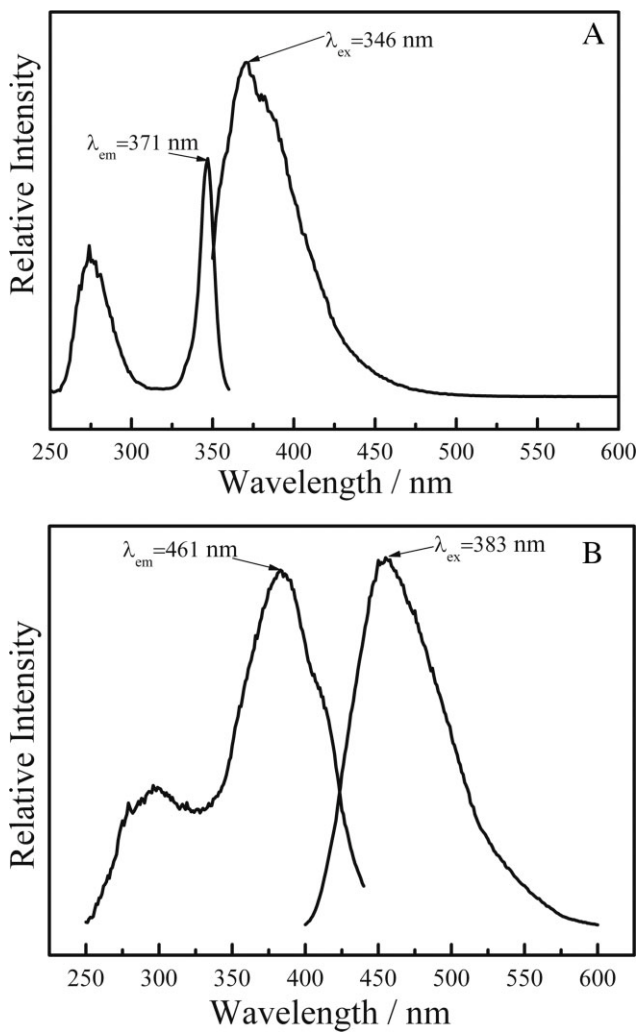

Figure 6 Emission–excitation spectra of PI monomer (A) and dedoped PPI (B) films. PPI films were prepared potentiostatically at 1.23 V versus SCE from BFEE. Solvent: DMSO.

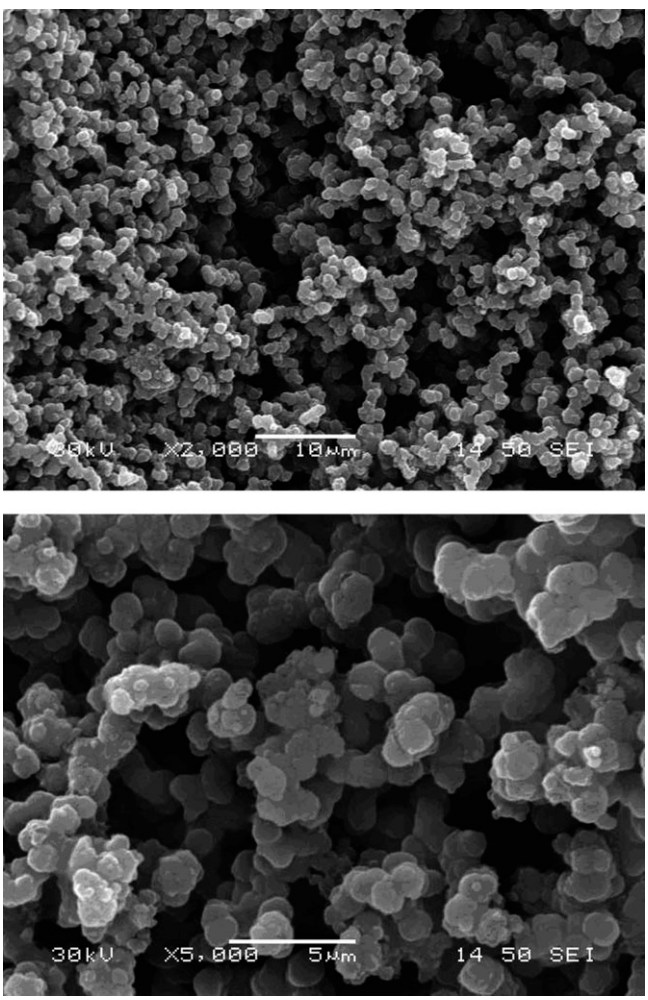

Figure 8 SEM micrographs of a PPI film deposited on the electrode surface from BFEE at a constant applied potential of 1.23 V versus SCE.

range of 285–1071 K at a heating rate of 10 K min^{-1}. According to Figure 7(A), there was a little bit of weight loss from 285 to 521 K, up to 8.64%, which can be ascribed to water evaporation or other moisture trapped in the polymer.[47] The second one occurred from 725 to 950 K, up to 12.06%, which was attributed to the degradation of the skeletal PPI backbone chain structure. In addition, there was still evident decomposition, about 4.15%, between 950 and 1061 K, possibly because of the overflow of some oligomers that decomposed from PPI with increasing temperature. From the thermal analysis, it can be reasonably concluded that PPI films prepared from BFEE owns good thermal stability.

Morphology and conductivity

The SEM images of a PPI film prepared in BFEE are shown in Figure 8. Macroscopically, PPI films that formed on a stainless steel anode were flat, compact, and metallic black in color. Microscopically, the polymer film resembled ordered arrangements of the granules. The growth of the nuclei was in the form of clusters. This morphology facilitated the movement of doping anions into and out of the polymer film during doping and dedoping, in good agreement with the good redox activity of PPI films.

The electrical conductivity of the PPI film obtained from BFEE was measured to be 10^{-2} S cm^{-1}, lower than that of a polyindole film (10^{-1} S cm^{-1}). These semiconducting properties will facilitate the applications of PPI films.

CONCLUSIONS

High-quality PPI films with an electrical conductivity of 10^{-2} S cm^{-1} were electrochemically synthesized in BFEE. The oxidation potential of PI in this medium was determined to be only 0.83 V, which was lower than that in ACN and 0.1 mol L^{-1} Bu_4NBF_4 (1.05 V). The as-formed PPI films showed good redox activity and high stability in BFEE. According to IR and theoretical calculations, the coupling between the monomer units occurred mainly at C_3 and C_6 positions. TGA results indicated good thermal stability for the PPI films obtained from BFEE. The fluorescence spectra suggested that soluble PPI was a blue-green light emitter.

References

1. Skotheim, T. A., Ed. Handbook of Conducting Polymers; Marcel Dekeker: New York, 1986.
2. Skotheim, T. A.; Elsembaumer, R. L.; Reynolds, J. R., Eds. Handbook of Conducting Polymers, 2nd ed.; Marcel Dekker: New York, 1998.
3. Wan, M. X. Gao Fen Zi Tong Bao 1999, 9, 47 (in Chinese).
4. Li, Y. F. Prog Chem 2002, 14, 207 (in Chinese).
5. Ghita, M.; Arrigan, D. W. M. Electrochim Acta 2004, 49, 4743.
6. Suematsu, S.; Ishikawa, T.; Hanada, M. Electrochemistry 2003, 71, 695.
7. Sazou, D. Synth Met 2002, 130, 45.
8. Billaud, D.; Maarouf, E. B.; Hannecart, E. Mater Res Bull 1994, 29, 1239.
9. Billaud, D.; Maarouf, E. B.; Hannecart, E. Synth Met 1995, 69, 571.
10. Pandey, P. C.; Prakash, R. J Electrochem Soc 1998, 145, 4103.
11. Abthagir, P. S.; Dhanalakshmi, K.; Saraswathi, R. Synth Met 1998, 93, 1.
12. Maarouf, E. B.; Billaud, D.; Hannecart, E. Mater Res Bull 1994, 29, 637.
13. Lazzaroni, R.; Depryck, A.; Debraisieux, C. H.; Riga, J.; Verbist, J.; Bredas, J. L.; Delhalle, J.; Andre, J. M. Synth Met 1987, 21, 198.
14. Yurtsever, M.; Yurtsever, E. Polymer 2002, 43, 6019.
15. Choi, K. M.; Kim, C. Y.; Kim, K. H. J Phys Chem 1992, 96, 3782.
16. Talbi, H.; Billaud, D. Synth Met 1998, 93, 105.
17. Tüken, T.; Düdükçü, M.; Yazlcl, B.; Erbil, M. Prog Org Coat 2004, 50, 273.
18. Waltman, R. J.; Diaz, A. F.; Bargon, J. J Phys Chem 1984, 88, 4343.
19. Zotti, G.; Zecchin, S.; Schiavon, G. Chem Mater 1994, 6, 1742.
20. Xu, J. K.; Nie, G. M.; Zhang, S. S.; Han, X. J.; Hou, J.; Pu, S. Z. J Polym Sci Part A: Polym Chem 2005, 43, 1444.
21. Xu, J. K.; Zhou, W. Q.; Hou, J.; Pu, S. Z.; Yan, L. S.; Wang, J. W. J Polym Sci Part A: Polym Chem 2005, 43, 3986.
22. Shi, G. Q.; Jin, S.; Xue, G.; Li, C. Science 1995, 267, 994.
23. Shi, G. Q.; Li, C.; Liang, Y. Q. Adv Mater 1999, 11, 1145.
24. Li, C.; Shi, G. Q.; Liang, Y. Q. J Electroanal Chem 1998, 455, 1.
25. Huang, Z. M.; Qu, L. T.; Shi, G. Q.; Chen, X. Y.; Hong, X. Y. J Electroanal Chem 2003, 556, 159.
26. Li, C.; Shi, G. Q.; Liang, Y. Q.; Ye, W.; Sha, Z. L. Polymer 1997, 38, 5023.
27. Wang, X. F.; Shi, G. Q.; Liang, Y. Q. Electrochem Commun 1999, 1, 536.
28. Wan, X. B.; Lu, Y.; Liu, X. R.; Zhou, L.; Jin, S.; Xue, G. Chin J Polym Sci 1999, 17, 99.
29. Xu, J. K.; Shi, G. Q.; Qu, L. T.; Zhang, J. X. Synth Met 2003, 135, 221.
30. Wang, X. F.; Xu, J. K.; Shi, G. Q.; Lu, X. J Mater Sci 2002, 37, 5171.
31. Wan, X. B.; Liu, X. R.; Xue, G.; Jiang, L. X.; Hao, J. J. Polymer 1999, 40, 4907.
32. Liu, C.; Zhang, J. X.; Shi, G. Q.; Zhao, Y. F. J Phys Chem B 2004, 108, 2195.
33. Wan, X. B.; Yan, F.; Jin, S.; Liu, X. B.; Xue, G. Chem Mater 1999, 11, 2400.
34. Li, C.; Shi, G. Q.; Liang, Y. Q. Synth Met 1999, 104, 113.
35. Wieder, H. H. Laboratory Note on Electrical and Galvanomagnetic Measurements; Elsevier Scientific Publishing Company: Amsterdam, 1979.
36. Zimmermann, C.; Mohr, M.; Zipse, H.; Eichberger, R.; Schnabel, W. J Photochem Photobiol A 1999, 125, 47.
37. Tasi, F. C.; Chang, C. C.; Liu, C. L.; Chen, W. C.; Jenekhe, S. A. Macromolecules 2005, 38, 1958.
38. Li, C.; Chen, F. E.; Shi, G. Q.; Xu, J. K.; Xu, Z. J. J Appl Polym Sci 2002, 83, 2462.
39. Lu, G. W.; Shi, G. Q. J Electroanal Chem 2006, 586, 154.
40. Lu, B. Y.; Xu, J. K.; Fan, C. L.; Jiang, F. X.; Miao, H. M. Electrochim Acta 2008, 54, 334.
41. Lu, B. Y.; Zeng, L. Q.; Xu, J. K.; Nie, G. M.; Cai, T. Acta Chim Sin 2008, 66, 1593.
42. Lu, B. Y.; Xu, J. K.; Fan, C. L.; Miao, H. M.; Shen, L. J Phys Chem B, In to appear.
43. Chan, H. S. O.; Choon, S. C. Prog Polym Sci 1998, 23, 1167.
44. Cihaner, A.; Onal, A. M. J Electroanal Chem 2007, 601, 68.

45. Cebici, F. C.; Sezer, E.; Sarac, A. S. Electrochim Acta 2007, 52, 2158.
46. Frisch, M. J.; Trucks, G. W.; Schlegel, H. B.; Scuseria, G. E.; Robb, M. A.; Cheeseman, J. R.; Montgomery, J. A., Jr.; Vreven, T.; Kudin, K. N.; Burant, J. C.; Millam, J. M.; Iyengar, S. S.; Tomasi, J.; Barone, V.; Mennucci, B.; Cossi, M.; Scalmani, G.; Rega, N.; Petersson, G. A.; Nakatsuji, H.; Hada, M.; Ehara, M.; Toyota, K.; Fukuda, R.; Hasegawa, J.; Ishida, M.; Nakajima, T.; Honda, Y.; Kitao, O.; Nakai, H.; Klene, M.; Li, X.; Knox, J. E.; Hratchian, H. P.; Cross, J. B.; Bakken, V.; Adamo, C.; Jaramillo, J.; Gomperts, R.; Stratmann, R. E.; Yazyev, O.; Austin, A. J.; Cammi, R.; Pomelli, C.; Ochterski, J. W.; Ayala, P. Y.; Morokuma, K.; Voth, G. A.; Salvador, P.; Dannenberg, J. J.; Zakrzewski, V. G.; Dapprich, S.; Daniels, A. D.; Strain, M. C.; Farkas, O.; Malick, D. K.; Rabuck, A. D.; Raghavachari, K.; Foresman, J. B.; Ortiz, J. V.; Cui, Q.; Baboul, A. G.; Clifford, S.; Cioslowski, J.; Stefanov, B. B.; Liu, G.; Liashenko, A.; Piskorz, P.; Komaromi, I.; Martin, R. L.; Fox, D. J.; Keith, T.; Al-Laham, M. A.; Peng, C. Y.; Nanayakkara, A.; Challacombe, M.; Gill, P. M. W.; Johnson, B.; Chen, W.; Wong, M. W.; Gonzalez, C.; Pople, J. A. Gaussian03, revision B.05; Gaussian, Inc.: Pittsburgh, PA; 2003.
47. Thieblemont, J. C.; Brun, A.; Marty, J.; Planche, M. F.; Calo, P. Polymer 1995, 36, 1605.